Optical design of the Developmental Cryogenic Active Telescope Testbed

Pamela S. Davila[a], Andrew E. Lowman[b], Mark E. Wilson[a], Rene A. Boucarut[a], Claudia M. LeBoeuf [a],
David C. Redding[b], Eric W. Young[a]

[a] – NASA Goddard Space Flight Center (GSFC), Greenbelt, MD 20771
[b] – Jet Propulsion Laboratory (JPL), 4800 Oak Grove Drive, Pasadena, CA 91109

ABSTRACT

In the summer of 1996, three study teams developed conceptual designs and mission architectures for the Next Generation Space Telescope (NGST)[1,2]. All three conceptual designs provided scientific capabilities that met or surpassed those envisioned by the Hubble Space Telescope (HST) and Beyond Committee[3]. Each group highlighted areas of technology development that need to be further advanced to meet the goals of the NGST mission. The most important areas for future study included: deployable structures, lightweight optics, cryogenic optics and mechanisms, passive cooling, and on-orbit closed loop wavefront sensing and control. NASA and industry are currently planning to develop a series of ground testbeds and validation flights to demonstrate many of these technologies. The Developmental Cryogenic Active Telescope Testbed (DCATT) is a system level testbed to be developed at Goddard Space Flight Center in three phases over an extended period of time. This testbed will combine an actively controlled telescope with the hardware and software elements of a closed loop wavefront sensing and control system to achieve diffraction limited imaging at 2 microns. We will present an overview of the system level requirements, a discussion of the optical design, and results of performance analyses for the Phase 1 ambient concept for DCATT.

Keywords: active optics, wavefront sensing, deformable mirror, segmented aperture, optical design, NGST

1. BACKGROUND

In all three of the design studies for NGST, the ability to sense and control the wavefront from the optical system to achieve diffraction limited imaging on-orbit was a key feature. Although wavefront sensing and control systems are currently an integral part of the design for many large aperture ground-based observatories, such as Keck and Gemini, the challenges presented by a space-based observatory are different. To some degree the design is easier because elaborate gravity compensation schemes do not have to be implemented and compensation for degraded imaging due to atmospheric turbulence is not a concern. On the other hand, the cold environment of space mandates the development of components and systems that will operate at low temperatures, typically 30 degrees Kelvin (for the L2 LaGrange point orbit). Mass constraints for reasonable launch vehicle envelopes drive the design of the optical telescope toward deployable, segmented, ultra-lightweight mirrors.. The wavefront sensing and control system must be able to detect and control optical wavefront errors resulting from deployment errors, and thermal gradients and vibrational modes coupled to the structural design of the system and to the spacecraft design.

Ideally, the wavefront sensing and control system could be an integral part of the science instrument module. For the GSFC concept presented in the summer of 1996, the wavefront sensing and control scheme included phase retrieval as a baseline method. This method of retrieving wavefront errors and detailed knowledge of the optical system from image data received great visibility during the early "trouble with Hubble" days. A number of noted experts in the field published papers during a frenzy of activity to determine the conic constant error on the Hubble Space Telescope primary mirror[4,5]. Image enhancement and phase retrieval methods have been proven by HST[6]. However, this method has not been proven to work for segmented aperture optical systems. This is one of the primary goals of our testbed development effort. Another goal is to explore the accuracy and fidelity of integrated modeling simulations by using these models to predict the performance of the real hardware system and by comparing these predictions with actual data[7]. In this way we will explore the limitations and capabilities of our baseline wavefront sensing and control technique. Another goal of the testbed activity is to have a calibrated optical system that can then provide a standard for future testing of other wavefront sensing and control techniques. The phased development of the DCATT testbed is discussed in detail in another paper[8]. During Phase I we focus on the development of an ambient system. The current plan is for the Phase I testbed to be integrated and operational during the second quarter of fiscal year 1999. Figure 1 is an illustration of the system concept for DCATT Phase I.

2. OVERVIEW OF THE SYSTEM, REQUIREMENTS, AND DESIGN APPROACH

The primary objective of the DCATT testbed is to represent in hardware an optical system that incorporates all of the functional elements envisioned in an NGST optical system. The NGST optical system will probably include an actively controlled, segmented primary mirror, actively controlled secondary, deformable, and fast steering mirrors, wavefront sensing optics and wavefront control algorithms. The goal for NGST is to use astronomical objects for guidance, target acquisition, and wavefront sensing, if possible. The functional block diagram in Figure 2 illustrates the components of the DCATT system and also highlights the key elements of hardware control. Like NGST, the DCATT system contains an actively controlled, segmented primary mirror, actively controlled secondary, deformable, and fast steering mirrors, wavefront sensing optics and wavefront control algorithms. In addition we have added a source module and a telescope simulator module to our system design. There are four modular components illustrated in Figure 2: (1) the source module, (2) the DCATT telescope, (3) the telescope simulator module, and (4) the Active Optics (AO) Bench module. The wavefront sensor hardware is also shown schematically on the bench. This hardware consists of a Dispersed Fringe Sensor (DFS), a CCD camera, and an Interferometric Wavefront Sensor (IWFS) (not shown in the diagram).

The top level requirement for the DCATT optical and control system is to demonstrate that diffraction limited imaging performance can be achieved at a wavelength of 2 microns under closed loop control. This translates to a corrected wavefront error goal of 1/14 wave rms at 2 microns or 1/4.45 wave rms at 633 nm. (The details of the error budget for both controlled and uncontrolled wavefronts are discussed in a separate paper[9].) The Phase I system is designed to operate at ambient temperature with a white light source (either Xenon or Tungsten) and with monochromatic laser sources as well. The optical bench and telescope structure is vibration isolated for interferometric measurements and for image stability. Mechanical and optical interfaces and fiducials on the optical bench will be defined to allow ease of integration of the system. Both the source module and the telescope simulator module will be kinematically mounted to the AO bench. The optical design approach was simplicity, reasonable cost within a limited budget, and, where possible, use of off-the-shelf, commercial, components. We selected a reflective optical design with a minimum number of elements to allow easy incorporation of infrared testing at a later date and to minimize chromatic effects.

The modular design approach depicted in Figure 2 was necessary to incorporate different optical configurations for alignment, calibration, and open and closed loop testing of the system. To check the alignment of the AO bench optics, the source module can be used directly with the AO bench optics and the CCD camera. Alignment verification and image quality measurements of the DCATT telescope will be achieved by using the source module with the telescope in double pass. Either a CCD camera can be installed at the focus of the telescope to directly record the images, or an interferometric test can be conducted. The telescope simulator module is designed for use with the source module for alignment verification of the AO bench optics and system level calibration of the active optical components and coarse and fine wavefront sensing hardware and software algorithms. The telescope simulator also allows testing of wavefront sensing and control algorithms with a range of aberration types and magnitudes not available with the telescope. Finally, the ultimate system level test will be with the source module plus the telescope in double pass and the AO bench optics in single pass. Final closed loop control of the system will be established in this configuration. Figure 3 is a schematic drawing showing the optical layout of the system for this configuration.

In Figure 3, the telescope is shown in an unfolded horizontal view. Light from the pinhole is reflected off a beamsplitter and then double passes the Cassegrain telescope optics. A Zerodur autocollimating flat mirror is used to double pass the telescope. In the actual use configuration, the telescope is mounted with its' optical axis oriented vertically and a fold mirror (not shown in figure 3) mounted on the AO bench directs the telescope beam along the horizontal axis toward the first off-axis parabola on the AO bench. This parabola acts as a collimator and also forms a real, accessible image of the exit pupil of the telescope onto the six inch diameter deformable mirror (DM), which is located in collimated space. The final off-axis parabola focuses the light at the desired output focal ratio, f/16.5. Both off axis parabolas are identical (diameter, effective focal length, and off axis distance) and are geometrically arranged to cancel the coma and astigmatism contributions from one another. A fast steering mirror (FSM) is included in the design for the purpose of experimenting with image stability and motion compensation when the bench is not vibration isolated and known disturbances are introduced. It may also be needed to correct low frequency modes in the telescope metering structure. Light from the final off-axis parabola is reflected from a beamsplitter and focussed onto the CCD camera. Light transmitted through the beamsplitter is imaged onto a quad cell for measurement of image centroid shifts. This information is fed back to the local control loop for the FSM. A pupil imaging mode is incorporated in the design to allow a direct measurement with the CCD camera of the pupil function (both geometry

and intensity) and to check the pupil alignment on the deformable mirror. This mode is obtained by inserting a pupil imaging lens in front of the CCD camera. (The pupil imaging lens is not easily seen in figure 3, because of its small size in the drawing.) The measured pupil data will be fed into the integrated model of the system.

Three types of wavefront sensors are designed for use with DCATT. A dispersed fringe sensor will allow us to measure large values of segment-to-segment piston errors and is designed to have a large dynamic range. Use of this coarse method of sensing should allow us to bring the wavefront errors to within 1 wave by adjusting the piston of the primary mirror segments. The CCD camera is mounted on a translation stage so that we can record both in-focus and out-of-focus images for phase retrieval. A multiple wavelength, phase shifting interferometric wavefront sensor will also be designed and built to characterize the final system performance.

3. TELESCOPE

After reviewing a number of different telescope designs, we finally settled on a two mirror, Cassegrain design for simplicity and ease of fabrication, alignment and test. The parabolic primary mirror design is segmented with a ring of six hexagonal segments arranged around a central segment. The size and shape of the segments was chosen for ease of fabrication and minimization of gravity sag, while being large enough to be of reasonable scale to the actuators and provide good angular step resolution through spacing of the actuators. The edges of the segments are separated by 6 mm gaps. The primary and secondary mirrors are diamond turned out of T6061 aluminum. Table 1 shows the first order design parameters and specifications of the telescope. The clear aperture of the f/2.2 primary mirror ended up being about 90 cm. The design goal for the telescope is to achieve diffraction limited imaging over a 2 by 2 arcminute field of view.

The Zerodur autocollimating flat will be mounted on a nine-point Hindle mount, which will in turn be mounted to a motorized jackscrew system having tip, tilt, and piston control. This feature will allow the flat to be directed off-axis to experiment with off-axis sources and phase diversity methods in the future. The flat will be polished to a 1/10 wave rms wavefront and coated with aluminum with a protective overcoat. The maximum gravity sag has been analyzed to be less than 40 nanometers peak-to-valley near the mounting points, with the effect dropping off rapidly away from these points.

4. AO BENCH OPTICS

Figure 4 is a drawing showing the AO Bench layout from a top view excluding the telescope. The deformable mirror (DM) must be able to compensate for wavefront aberrations introduced by a variety of elements in DCATT. The displacement, location and positioning of the actuators will have a direct effect on the ability to control and compensate wavefront errors. For attaining low aberrations and optimum performance, the deformable mirror must be able to compensate for up to 8 _m of wavefront errors over its field of view with control of the wave errors in 4 nm steps. We have assumed that the actuator's stroke is one-half of the wavefront error so the actuator's stroke will be at least 4 _m with incremental steps of 2 nm. For achieving the desired wavefront control, we require the actuator's uniformity and linear response (voltage vs. displacement) to be within five percent and the hysteresis in the actuator's position to be less than one percent. The frequency response for the DM will be at least 1kHz. We require, over the clear aperture area of the DM, a surface finish of 15 Angstroms rms or better and a figure of _/14 rms at 633 nm. The mirror reflectivity will be greater than 85% from 400 nm to 2000 nm. The 903-mm diameter of DCATT's primary mirror is mapped to a clear aperture on the DM of 124 mm. For an actuator spacing of 7 mm, we sample the pupil image with about 17 actuators per axis (or roughly about 5 actuators per segment). The Xinetics DM we are procuring for DCATT has a square grid pattern of 349 PMN (lead magnesium niobate) piezo-electric actuators.

The fast steering mirror requirements are still under investigation. Our current thinking is that the device bandwidth will be on the order of a few hundred Hertz, with a range adequate to handle drift and DC offset errors as well as any low frequency modes that may be excited in the metering structure. A quad cell will provide closed loop feedback to the fast steering mirror.

4.1 Source Module

Figure 5 is a diagram of the components in the source module. Initially we will configure the system to work with either white light or a 1 milliwatt frequency stabilized HeNe laser. The white light source is a 75 Watt Xenon arc source used with a condenser lens and a convectively cooled housing with heat straps. Although the Oriel Xenon source has some strong emission lines above 800 nm, this source is stronger in total radiance output than the alternate source considered, a 10 W

Tungsten Halogen bulb. We will also be buying the Quartz Tungsten Halogen source for experimentation. Three, five position filter wheels are shown in the sketch: two at the output of the white light source and one at the output of the laser source. The white light source will have an ND filter set and a narrowband spectral filter set especially designed for optimum recovery of wavefront errors using phase retrieval. Our current conception of the types of spectral filters we would need for testing includes: 633 ± 0.5 nm, 633 ± 5.5 nm, and 633 ± 20 nm. The last two positions on the spectral filter wheel will be opened and closed positions. When the white light source is used, the 5 micron pinhole and the 20 micron pinhole are both in the beam path. These two were sized to produce a diffraction limited source centered at about 633 nm. A mechanized rotating polarizer (not shown) will also be used in the laser beam path to allow continuous variable remote control of the laser intensity.

4.2 Telescope simulator module

Figure 6 shows the layout of the telescope simulator module. When used with the source module, the telescope simulator module will provide a calibrated, controllable source. The telescope simulator module is designed to simulate the following types of optical wavefronts: (a) continuous, aberrated wavefront, (b) segmented, aberrated wavefront, (c) segmented, unaberrated wavefront, and (d) continuous, unaberrated wavefront. Transmissive phase plates used in double pass will provide a method of introducing known, calibrated amounts of piston error into the wavefront and thus allow us to characterize the dynamic range and accuracy of the dispersed fringe sensor and the wavefront sensor. A small deformable mirror with 69 actuators will be used to generate aberrated wavefronts. A flat mirror can be inserted in front of the deformable mirror to bypass this active element.

The telescope simulator exit pupil is designed to match the DCATT telescope exit pupil size and distance from the paraxial focal plane. Thus, when the simulator is used with the AO bench optics, the pupil images will be imaged onto the DM in the AO bench in the same place and position as the DCATT telescope pupil. We will not have to re-align the AO bench DM when we switch between the simulator and the DCATT telescope. The deformable mirror in the telescope simulator will allow us to dial in certain known amounts of aberrations (characterized with a ZYGO interferometer first) and then to test the ability of the AO bench DM to compensate for these known aberrations. We will be able to systematically study and quantitatively measure the performance of the system.
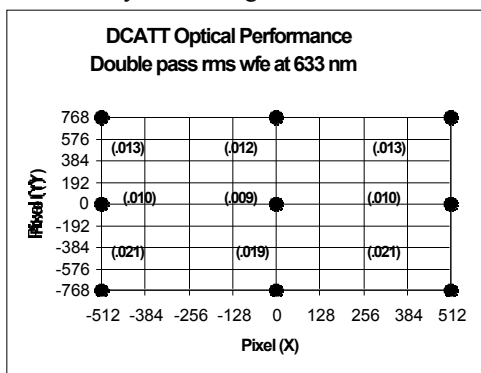
4.3 Wavefront sensors

The baseline system for coarse detection of piston errors between the segments is a Dispersed Fringe Sensor (DFS). This method has been implemented for phasing of the Palomar Testbed Interferometer and as a breadboard beam combiner for the Space Interferometry Mission. If you combine the wavefront from two identical segments with only piston error between them, you get an Airy disk that is modulated by the cosine of the phase (in waves). If you write the cosine in terms of the physical piston (in microns), the cosine argument goes as $1/\lambda$. The DFS spreads out the spectrum so that ideally $1/\lambda$ is linear in space, i.e., converting cosine $(1/\lambda)$ to cosine (x). The current dispersed fringe sensor is a grism design with a BK7 substrate and a replicated diffraction grating with a groove density of 35 lines/mm on the back surface. When the DFS is in the beam, the CCD camera will be used to record the fringe pattern. The CCD camera can be translated in the focus direction, if required. Figures 7 and 8 show typical image data output from the DFS. In theory, the DFS should allow us to measure many waves of piston error between neighboring segments and then adjust the actuators on the primary mirror segments to minimize the error. The goal is to get the wavefront error to within 1 wave with this technique and then use the phase retrieval to reduce the wavefront errors even further by activating both the segments (if required) and the deformable mirror.

The CCD camera in our design has multiple uses. It can be used to record field or pupil images (pupil images if the pupil imaging lens is inserted in the path), or to record interference fringes from the dispersed fringe sensor. The camera is mounted on a one-axis translation stage with a total range of ± 50 mm. After performing a survey of commercial scientific grade cameras, we selected a Photometrics model with a Kodak 1600 chip. The array size is 1536 x 1024 with 9 micron square pixels. With the 14 bit digitizer we have the option of binning pixels to improve dynamic range at the expense of resolution, if desired. This is done on-chip to add the signals without adding the read noise, hence a real improvement in dynamic range. The camera has a thermoelectric cooler and a liquid circulation unit and operates optimally between – 25 and – 40 degrees Centigrade with typical low read noises of 12 – 15 electrons and typical dark currents of 0.03 – 0.005 electrons/photon/second. A PCI interface and a software library come with the camera.

As a future addition to the system, a phase shifting interferometer (the Interferometric Wavefront Sensor shown in Figure 4) used at multiple wavelengths (probably 633, 612, and 543 nm) will enable us to measure the segment phasing errors as well as their individual figures.

5.   RESULTS OF PERFORMANCE ANALYSIS

The performance of the optical system, with the telescope in double pass and all other optics used in single pass mode, was determined by evaluating the rms wavefront error at 633 nm as a function of position on the detector. The corner pixel (512,768) corresponds to a field point of 1.6 x 1 arcminute with a platescale of 8.5 arcsec per pixel. The primary off axis aberration is coma, introduced by the Cassegrain telescope. There is residual field curvature but this is well within the diffraction depth of focus (± 0.25 mm). The attached figure shows the performance data.

DCATT Optical Performance
Double pass rms wfe at 633 nm

Pixel (Y)			
768	(.013)	(.012)	(.013)
0	(.010)	(.009)	(.010)
-768	(.021)	(.019)	(.021)

Pixel (X): -512 -384 -256 -128 0 128 256 384 512

6. SUMMARY AND ACKNOWLEDGEMENTS

The detailed optical design is almost complete and we are in the process of procuring the components. An experimental test plan and overall test, alignment, and integration plan is being completed for the DCATT system.

We would like to take this opportunity to thank the following individuals who have been extremely helpful in the DCATT effort: Howard Hall and Dave Jacobsen (Marshall Space Flight Center), Dan Coulter (Jet Propulsion Laboratory), and Bernie Seery and Paul Geithner (Goddard Space Flight Center). Special thanks to the mechanical engineers and designers: Jamie Britt, Dave Robinson, Rick Fedorchak (Goddard Space Flight Center) and Tom Hanyok (Swales Aerospace, Inc.).

7. REFERENCES

[1] TRW NGST Final Study Report, TRW, 1996.

[2] Lockheed Martin NGST Final Study Report, LMMS/PO86946, August 1996.

[3] "Exploration and the Search for Origins: A Vision for Ultraviolet-Optical-Infrared Space Astronomy, Report of the HST and Beyond Committee, ed. A. Dressler, AURA, 1996.

[4] J. R. Feinup, J. C. Marron, T. J. Shulz, and J. H. Seldin, "Hubble space telescope characterized by using phase-retrieval algorithms," Appl. Opt. **32**, pp. 1747-1767, 1993.

[5] D. Redding, P. Dumont, and J. Yu, "Hubble space telescope prescription retrieval," Appl. Opt. **32**, pp. 1728-1736, 1993.

[6] R. G. Lyon, J. E. Dorband, and J. M. Hollis, "Hubble Space Telescope Faint Object Camera calculated point-spread functions", Appl. Opt. **36**, pp. 1752-1765, 1997.

[7] D. C. Redding, S. A. Basinger, A. E. Lowman, A. Kissil, P. Y. Bely, R. Burg, G. E. Mosier, M. Femiano, M. E. Wilson, D. N. Jacobson, J.Rakoczy, "Wavefront sensing and control for a next generation space telescope", *Proc. of SPIE, Space Telescopes and Instruments V,* **3356**, 1998.

[8] C. M. LeBoeuf, P. S. Davila, D. C. Redding, A. Morell, A. E. Lowman, M. Wilson, E. W. Young, L. K. Pacini, and D. R. Coulter, "Developmental cryogenic active telescope testbed, a wavefront sensing and control testbed for the Next Generation Space Telescope", *Proc. of SPIE, Space Telescopes and Instruments V,* **3356**, 1998.

[9] E. W. Young, M.E. Wilson, P. S. Davila, W. Eichhorn, C. M. LeBoeuf, D. C. Redding, A. E. Lowman, "Performance analysis of the developmental cryogenic active telescope testbed (DCATT)", *Proc. of SPIE, Space Telescopes and Instruments V,* **3356**, 1998.
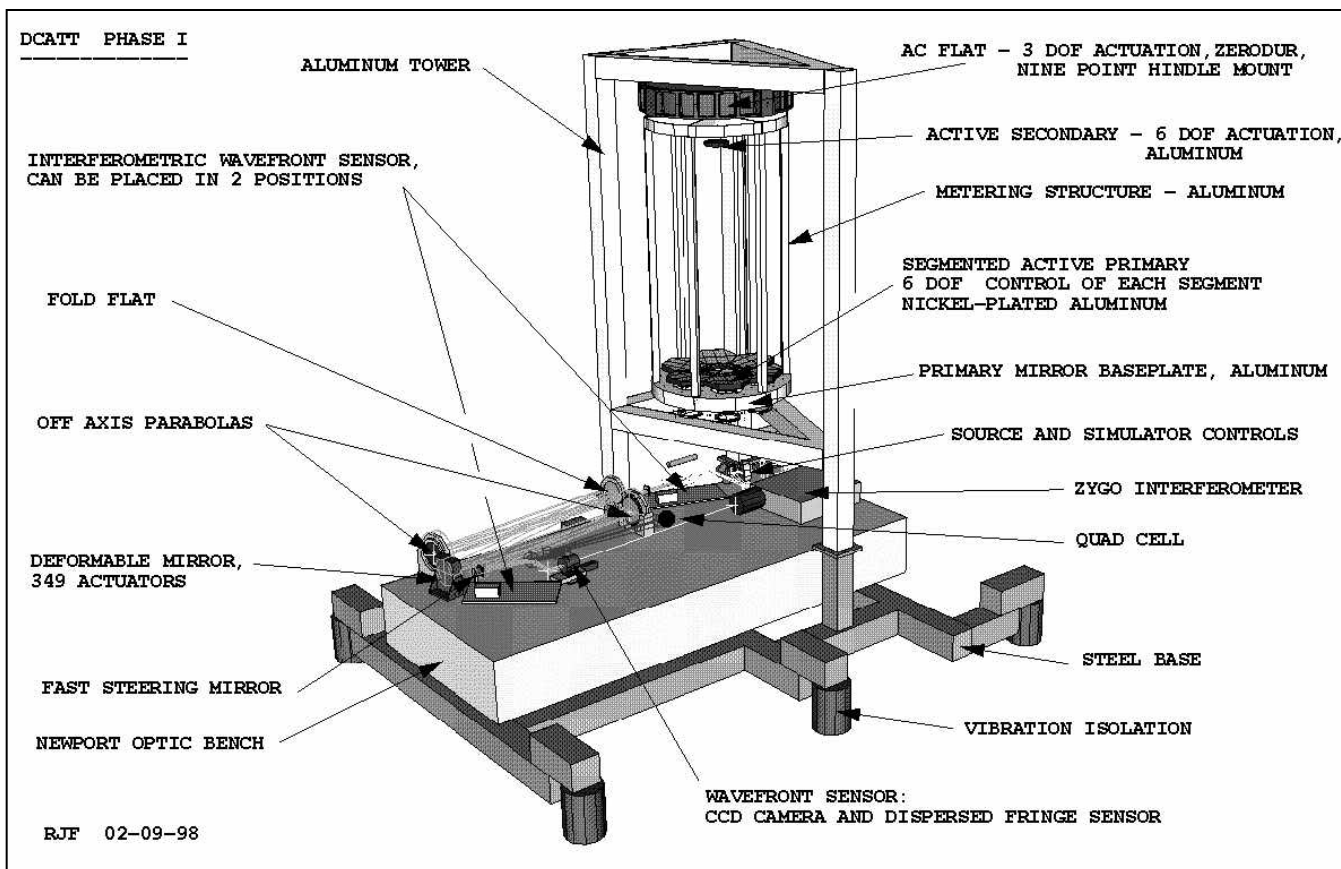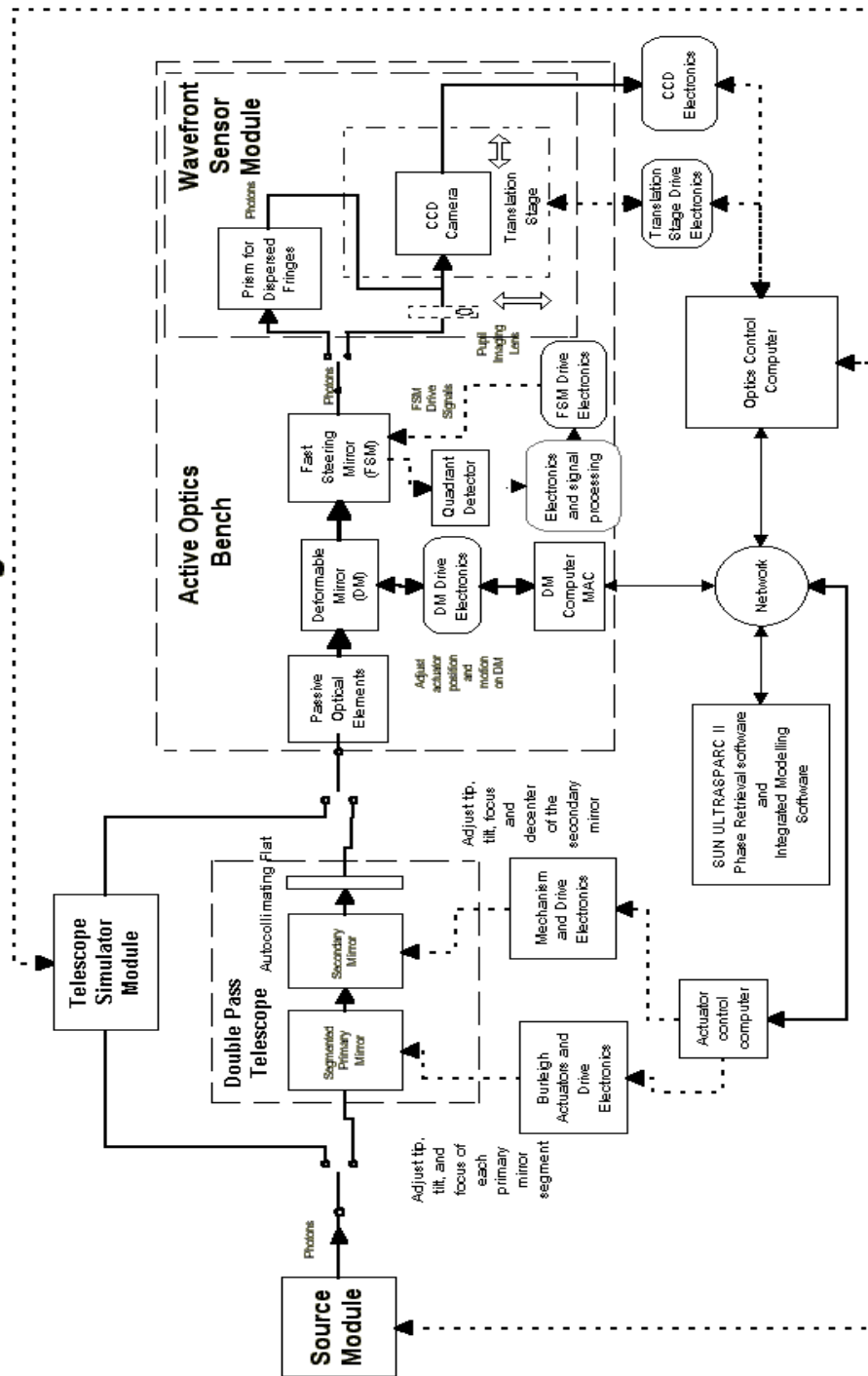
Figure 1. Overview of the DCATT Phase I system. Drawing courtesty of Rick Fedorchak, Goddard Space Flight Center.

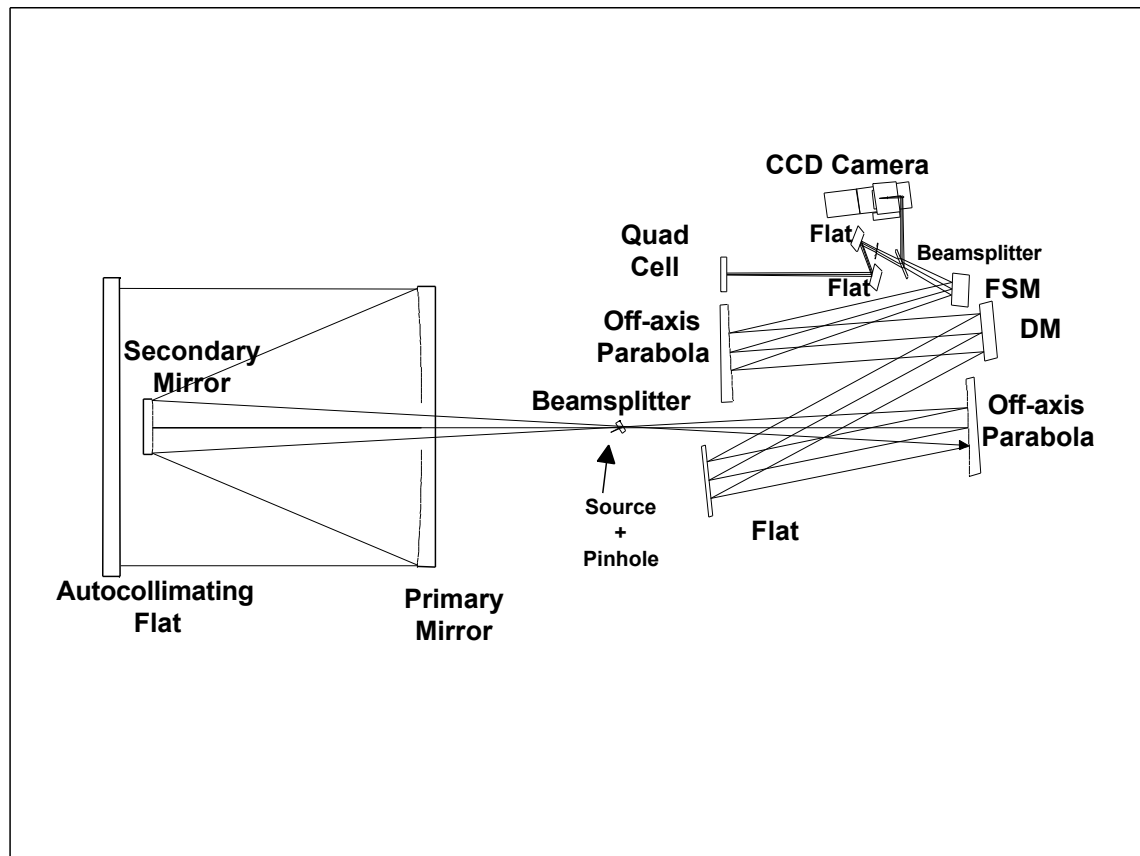Figure 2. DCATT functional block diagram.

Figure 3. Layout of the DCATT configuration - Source + double pass telescope + AO bench. Note primary mirror not shown as segmented.

Telescope	Parameter
Primary mirror clear aperture diameter	903mm (Aperture stop at primary mirror)
Primary mirror f/number	2.2
Telescope f/number	16.6
Telescope back focal distance (from primary vertex to image)	1250 mm
Primary to secondary intervertex distance	1617.637 mm
Secondary mirror clear aperture diameter	174 mm
Secondary mirror magnification	7.5
Overall Length (from telescope secondary to paraxial image plane, unfolded)	2867.639 mm
Design wavelength	632.8 nm
Exit pupil diameter	193.5 mm
Exit pupil location(distance from paraxial image plane toward secondary)	3214 (mm)
Total field of view	3.16 x 2.10 arcminutes
Primary mirror hole cutout diameter (for unvignetted field of view)	84 mm
Obscuration ratio	0.2
Aft Optics	
Overall length (from telescope image to OAP 1 clear aperture center)	2039.139 mm
Overall Width	944 mm
OAP Focal Length	2032 mm
OAP1 and OAP2 clear aperture diameters	164 mm
Fold flat diameter	155 mm (Circular, Active Area)
DM Diameter	137 mm (Circular, Active Area)
FSM Diameter	56 mm (Circular, Active Area)
System	
F/number	16.6
Exit Pupil Diameter	438 mm
Exit Pupil Location (distance from CCD to final exit pupil)	7300 mm

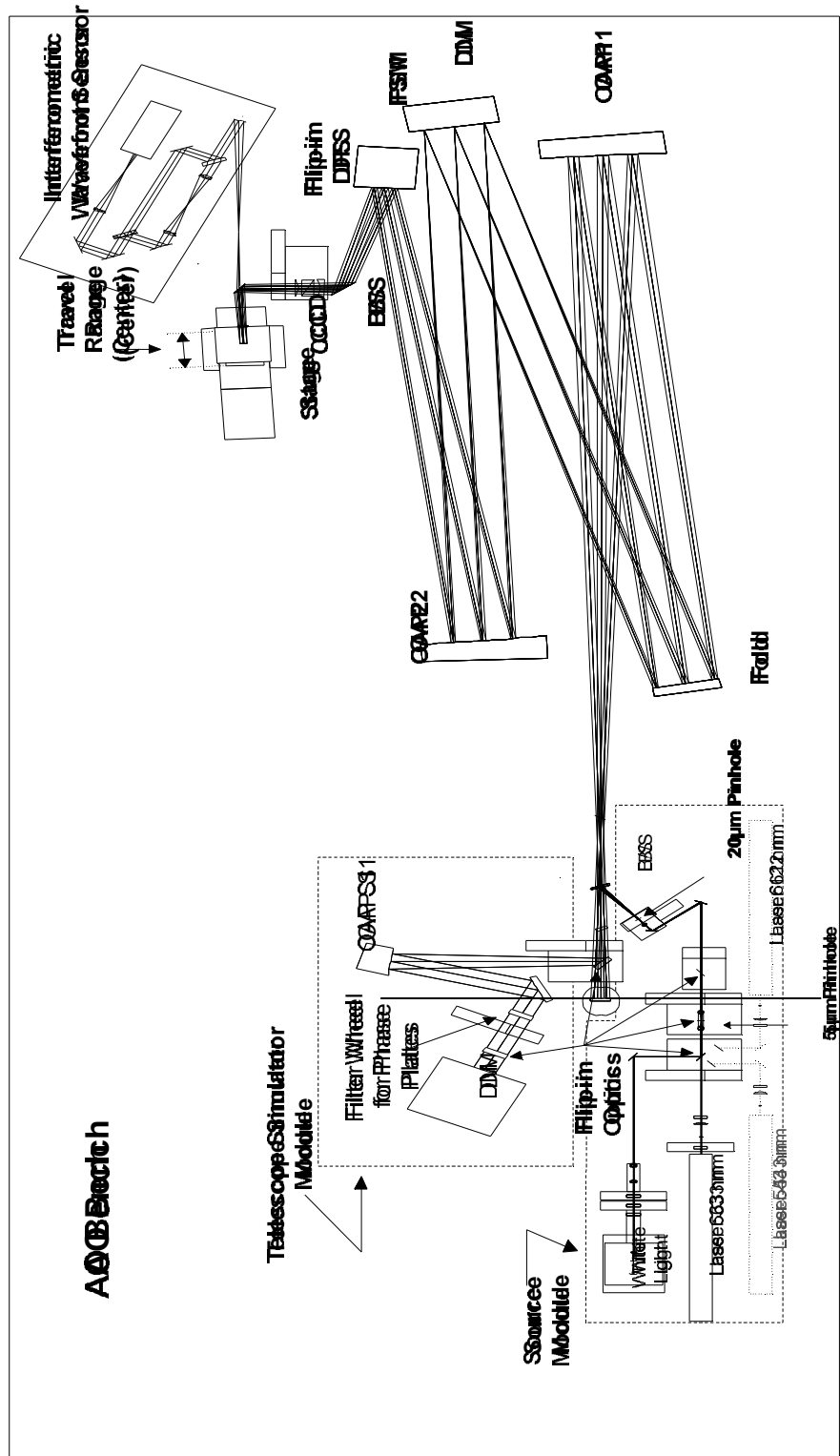**Table 1. First order design parameters for the DCATT telescope, aft-optics and system.**

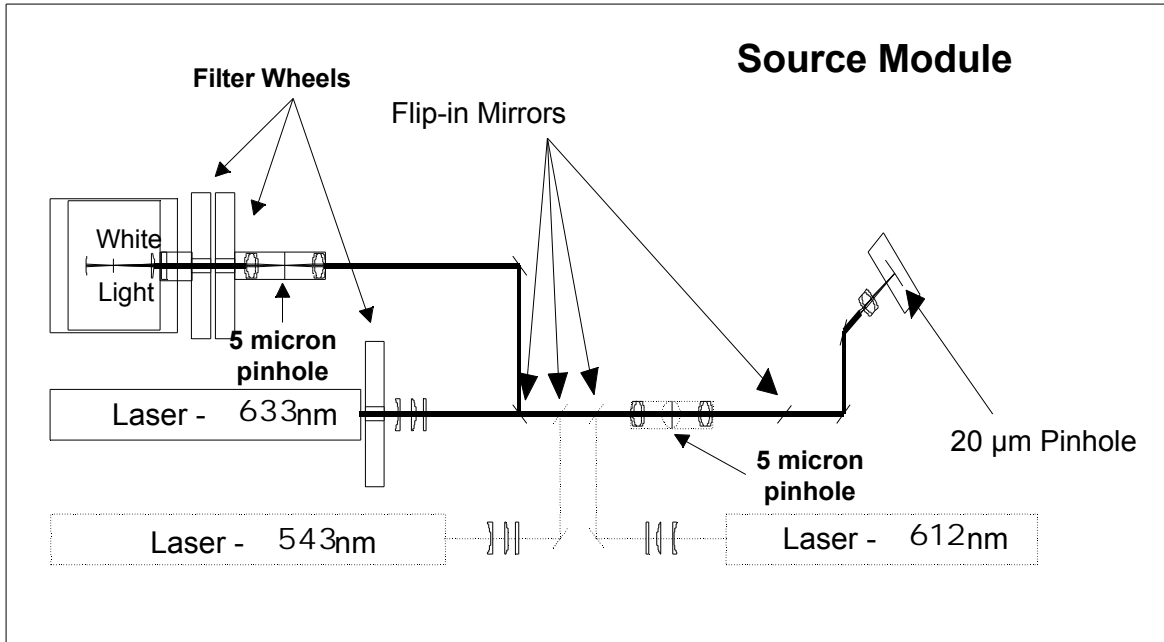**Figure 4. Top view of the DCATT AO bench, excluding telescope.**

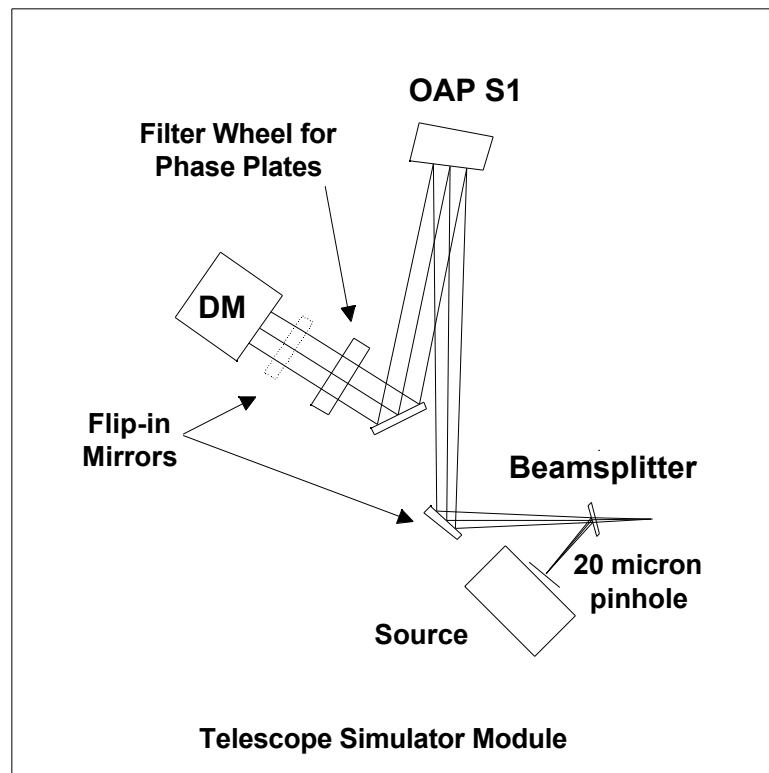**Figure 5. Layout of the optics in the source module.**

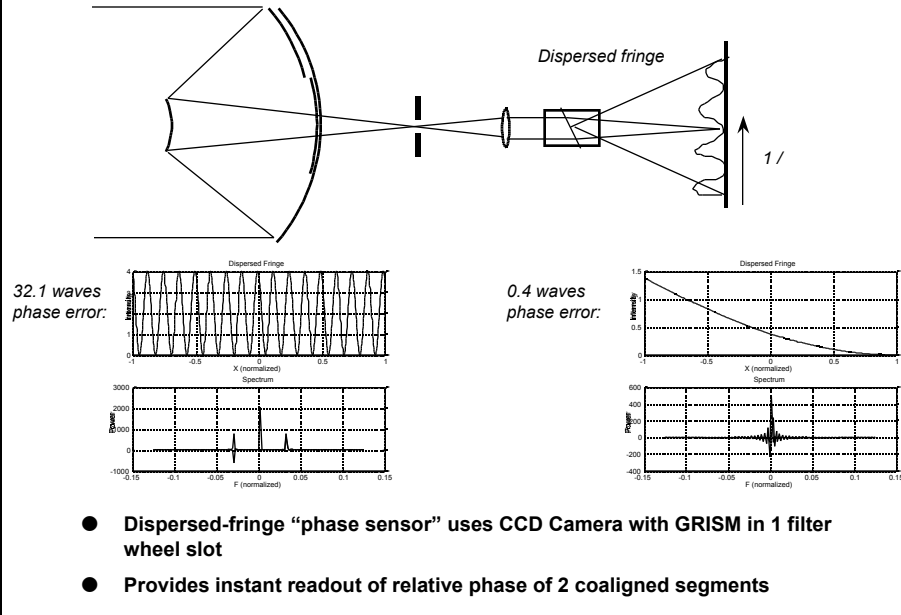**Figure 6. Layout of the optics in the telescope simulator module.**

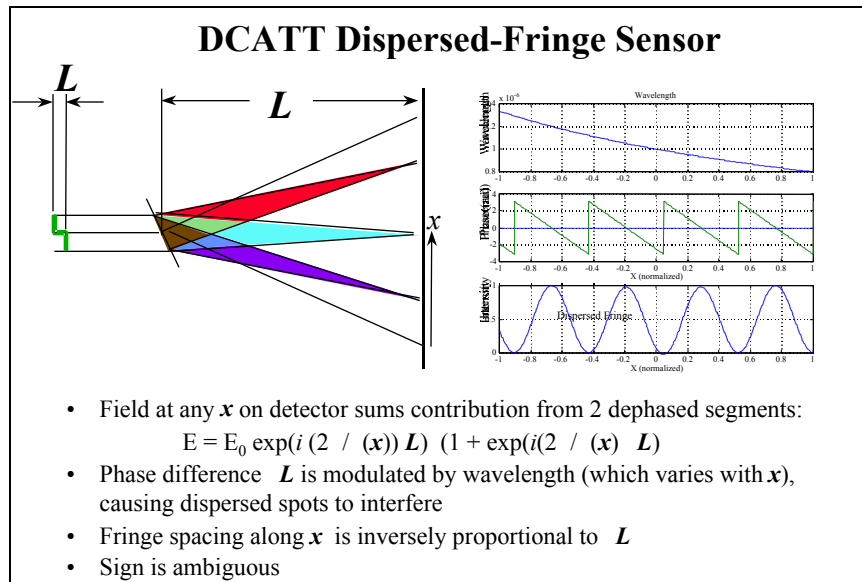**Figure 7. Coalignment and cophasing of the primary mirror segments using the Dispersed Fringe Sensor.**

Figure 8. Theory of operation of the dispersed fringe sensor.